# Development of "Cavitons" and Trapping of rf Field*

H. C. Kim,† R. L. Stenzel and A. Y. Wong
*Department of Physics, University of California, Los Angeles, California 90024*
(Received 18 March 1974)

A new kind of parametric instability is observed in a nonuniform plasma in which a resonant rf electric field and a density cavity grow simultaneously through mutual enhancements. The threshold is observed to be virtually zero and the growth rate is linearly dependent on pump intensity, $E_0^2$. Ponderomotive force and wave trapping are observed to be the mechanisms which drive the instability.

We wish to report an observation of a new kind of parametric instability in a driven nonuniform plasma with a pump electric field directed parallel to the density gradient. The ponderomotive force[1] of the linearly enhanced electric field[2] first generates a density cavity[3] at the resonant location, $\omega_{pe}(z_0)=\omega_0$. The cavity in turn traps the rf field and causes mutual enhancements between the rf field and the density perturbation.

The experiment is performed in a unmagnetized dc-discharge plasma produced in a vacuum chamber of 60 cm length and 30 cm diam with base pressure $2\times10^{-7}$ Torr [Fig. 1(a)]. The axial density gradient is produced by distributing hot filaments in only one half of the chamber. Typical parameters are argon pressure $3\times10^{-4}$ Torr, $n_0\approx10^9$ cm$^{-3}$, noise level $n/n_0\lesssim0.1\%$, $n_0/(dn_0/dz)=20$ cm, $T_e=1$ eV, $T_i=0.1$ eV, and $\nu_{en}/\omega_0\approx3\times10^{-3}$. A quasistatic external rf field ($\omega_0/2\pi=360$ MHz) is imposed on the plasma by an electrode located at the low-density region in the chamber; the excited region is well separated from the exciter on account of the density inhomogeneity. The amplitude of this external field $E_0$ decreases exponentially (scale length $\approx4$ cm) along the axial direction as a result of the finite size of the exciter. We have used the following "remote" diagnostic techniques: An electron-beam probing technique[4] [Fig. 1(a)] to measure the rf field, a thin Langmuir probe to measure the density perturbation which propagates out after the rf is terminated, and a small rf resonant dipole probe [Fig. 1(b)] to supplement the electron-beam technique. Comparisons between the two methods are summarized in Table I.

The steady-state field $E_T$ in the plasma is monitored by observing the lateral spread of a narrow (0.5 mm diam) electron beam (5–9 keV, 0.1 $\mu$A, $n_b=10^4$ cm$^{-3}$) traversing the resonant region along the radial direction in approximately $\frac{1}{2}$ to $\frac{1}{4}$ of the rf period. Using the probe to map out the radial extent of the resonant region ($\Delta r\simeq5$ cm) and taking into account the amplification of the electron beam deflection in the drift space, we establish the correlation between the rms value of $E_T$ and the maximum lateral spread of the electron beam ($E_T=5$ V/cm per 1 mm spread). The phase relationship between the total field $E_T$ and the externally imposed field $E_0$ is conveniently measured by generating Lissajous figures. The electron beam is modulated vertically by $E_0\times\cos\omega_0 t$ through a set of plates at the source and after the horizontal modulation by the resonant

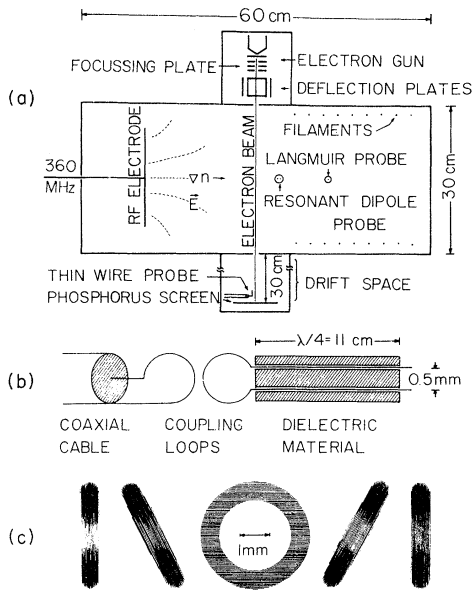


FIG. 1. (a) Schematic diagram of the apparatus, showing plasma device and differentially pumped electron beam device. (b) Resonant-dipole probe consisting of a $\lambda/4$ resonator in a ceramic shield. The potential difference measured between the exposed probe tips is magnetically coupled to a 50-$\Omega$ coaxial cable. (c) Sketches of the observed variation of the Lissajous pattern when the density is increased: (from left to right) $\omega_{pe}^2(z_0)/\omega_0^2=0.85$, 0.97, 1.00, 1.03, and 1.10. $P_0=10$ W, $\omega_0/2\pi=360$ MHz, steady state. The horizontal deflection is caused by the plasma field and the vertical deflection by a constant external field.

TABLE I. Comparisons of electron-beam and resonant-dipole-probe diagnostic techniques of measuring rf fields.

| | Electron beam | Resonant-dipole probe |
|---|---|---|
| Location of resonant region | No disturbance for low-intensity beams | Shifted up to 2 cm toward higher density side[a] |
| Resonant width | 1 cm = $20\lambda_D$ | Broadened to 2 cm[a] |
| $E_T/E_0$ at resonance[b] | Steady state: 30<br>Peak: 100 | Steady state: 3<br>Peak: 10[a] |
| Frequency response | dc to 1 GHz | Limited |

[a]Because of the sheath near the probe. The sheath also could produce high- and low-frequency noise. The probe also exhibits spurious resonant probe effects.

[b]Ordinary single-wire probes give much lower readings.

field $E_T\cos(\omega_0 t+\varphi)$ it emerges on the phosphorus screen as a Lissajous figure whose ellipticity depends on $E_T$ and $\varphi$ [Fig. 1(c)]. The temporal and spatial development of the rf field $E_T$ and the corresponding density perturbation $\delta n$ are studied by pulsing on the external field $E_0$ [Fig. 2(a)]. The time-resolved beam measurements employ a sampling technique whereby short pulses (200 nsec) of the 9-keV electron beam are injected repeatedly into the resonant region at the desired times and the beam spread is monitored either visually on the phosphorus screen or electronically with a thin wire probe (0.5 mm diam). High sensitivity is achieved by modulating the beam intensity slowly (500 Hz) and using phase-sensitive detection technique. Since the density measurement with a Langmuir probe in the presence of the large-amplitude rf field is subject to serious error by sheath rectification, the pump field is turned off at the desired time and the density is determined 1 $\mu$sec later, which is sufficiently long for the rf field to decay but short on the time scale of the density relaxation.

The time- and space-resolved measurements show simultaneous exponential growth of $\langle E_T^2\rangle$ and $\delta n$ at the resonant location [Fig. 2(a)], with the growth rate $\gamma$ depending linearly on the pump power $E_0^2$ [Fig. 2(b)]. Measurements of the absolute rf field strength and density perturbation establish $\delta n \propto \langle E_0^2\rangle$ qualitatively and $\langle E_T^2\rangle/8\pi n_0\kappa T_e \approx \delta n/n_0$ quantitatively within 30% error. For a 10-W pulsed pump ($E_0 \approx 0.5$ V/cm), $\langle E_T^2\rangle/8\pi n_0\kappa T_e$ grows to a saturated value of 25% in about 10 $\mu$sec which is the typical time scale for the development of the ion density perturbation. This time scale required for saturation is almost independent of the pump power for $E_T^2/4\pi n\kappa T_e \lesssim 0.2$. The resonant width at this time is typically 1 cm or 20 Debye lengths.[5] The behavior of $\langle E_T^2\rangle$ and $\delta n$ after the saturation depends on the density gradient scale length: For gentle density gradient ($k_D L > 500$), $\langle E_T^2\rangle$ and $\delta n$ break down into several peaks and propagate out from the resonant region towards regions of higher and lower densities[6]; for steeper density gradient ($k_D L < 500$), a short-wavelength ($k\lambda_D = 0.3$) ion acoustic wave is generated inside the density cavity

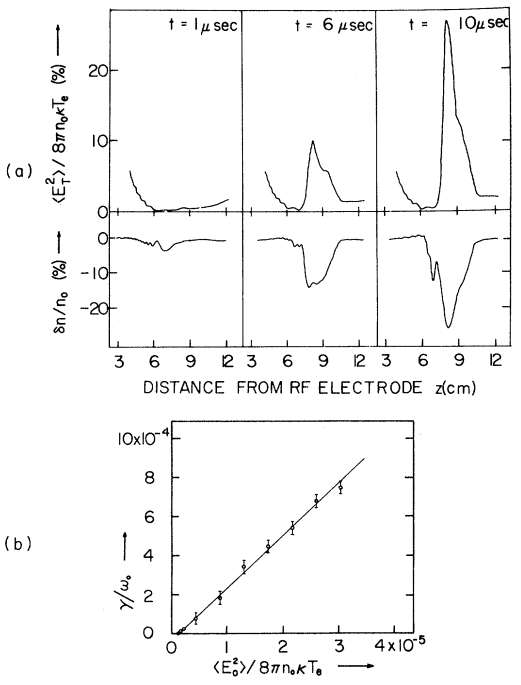


FIG. 2. (a) Profiles of the normalized field intensity (top traces) and density perturbation (bottom traces) at different times $t$ after turn-on of 10-W rf pump (measured with probe). rf pressure and density perturbation mutually enhance each other. (b) Growth rate of $\langle E_T^2\rangle$ versus applied pump intensity $\langle E_0^2\rangle$.

and propagates down the density gradient. When the ion acoustic wave is generated, $\langle E_T^2 \rangle$ in the density cavity oscillates at the ion acoustic frequency (~1 MHz) and starts to decay to the final steady-state value, approximately $\frac{1}{10}$ of the peak value. The temporal behavior of $E_T$ is measured with both the rf probe and the electron beam, and the same qualitative behavior is found. The result shows that for a 10-W pulsed pump, the beam spread reaches the peak value of 1 cm at 10 $\mu$sec while the steady state beam spread decreases to 3 mm. The beam also exhibits oscillatory states near the saturated value. The absolute measurement of $E_T$ is presented in Table I.

In spite of the large density perturbations the resonant rf field keeps on growing in the vicinity (within 2 cm) of the initial resonant location indicating that the rf field is trapped inside the density cavity.[7] In order to verify this hypothesis, we turned off the rf pump abruptly (0.3 $\mu$sec fall time) and studied the temporal decay of $E_T$ inside the density cavity by the electron-beam technique. Because the smaller electron-neutral collision rate at lower pressures favors this observation, the following parameters have been chosen: Ar pressure $5\times10^{-5}$ Torr, $\omega_0/2\pi = 100$ MHz, $\nu_{en}/\omega_0 \approx 10^{-3}$, and $L = n_0/(dn_0/dz) = 40$ cm. In the absence of the wave trapping, the rf field would convect out of the resonant region on the time scale

$$t = \int_{z_0}^{z_0-\Delta z} dz/v_g(z) = 200 \text{ nsec},$$

where

$$v_g(z) = [(3\kappa T_e/m_e)(z_0 - z)/L]^{1/2}$$

is the local group velocity and $\Delta z$ is the resonant width, while with trapping the rf field decays on the time scale of the electron-neutral collision (1.6 $\mu$sec). A strong pump field (15 W) is pulsed with duration (1 $\mu$sec) just long enough to produce the enhanced field inside the density cavity. The subsequent slow decay of $E_T$ (time constant $\tau = 1.5$ $\mu$sec) indicates collisional decay of the trapped plasma oscillations [Figs. 3(a) and 3(b)]. The density profile monitored immediately after the end of a short rf pulse shows a density barrier on both sides of the density cavity as expected from the expulsion of particles by the ponderomotive force. This configuration is particularly favorable to the trapping of plasma waves and explains the enhancement of rf field in the presence of a density cavity. After turning off the rf pulse, the density cavity propagates with initial velocity approximately 4 times sound speed and slows down to sound speed as the amplitude becomes smaller [Fig. 3(c)].

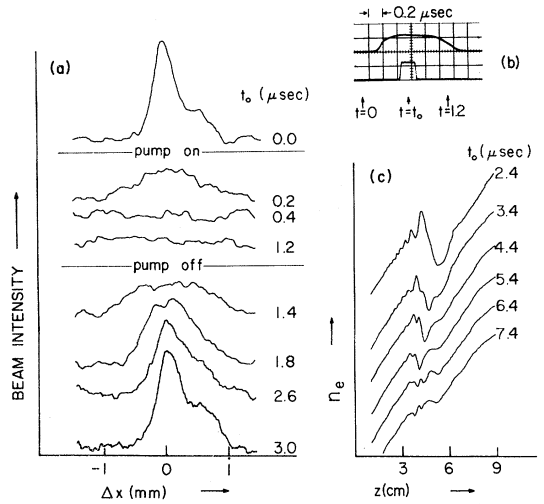


FIG. 3. (a) Temporal evolution of the beam deflection before, during, and after the rf excitation. (b) The time resolution is achieved by switching the 9-keV electron beam on only during the desired time. Upper trace shows $\langle E_0^2 \rangle$ versus $t$. Lower trace shows the pulse during which the electron beam is switched on. (c) Relaxation of the density cavity after the pump is turned off.

The observed mutual enhancement between the rf field pressure and the stationary density perturbation is a characteristic of the oscillating two-stream instability.[8] However, the presence of the density gradient initiates a spatially localized rf field and a density perturbation from which the instability grows. This explains why the threshold field of this instability ($\langle E_0^2 \rangle/8\pi n_0 \kappa T_e \approx 10^{-6}$) is much smaller than the threshold of the oscillating two-stream instability in uniform plasmas[9] ($\langle E_0^2 \rangle/8\pi n_0 \kappa T_e \approx 10^{-3}$).

Based on our experimental results the following physical picture emerges: The applied rf field $E_0$ is enhanced by the process of linear conversion to electrostatic modes, whose field is maximum at the resonant location where $\omega_{pe} \approx \omega_0$. The rf field enhancement is limited by the convective loss of electron plasma waves out of the resonant region. The density cavity created by the ponderomotive force of this enhanced rf field favors trapping of the rf field and the convective loss is reduced. This results in a higher rf field which in turn creates a deeper density cavity and the process continues until saturation mechanisms set in. A computer simulation of our experiment also shows the creation of the density well and

the wave trapping.[10]

We gratefully acknowledge helpful discussions with Dr. J. M. Dawson, Dr. Y. C. Lee, Dr. G. Morales, and Dr. K. Nishikawa. The electron beam apparatus was constructed by Mr. B. H. Quon with the gun obtained by the courtesy of Tektronix Inc. The indispensable help of Mr. Z. Lucky is deeply appreciated.

---

*Research supported by the U.S. Air Force Office of Scientific Research under Grant No. AFOSR 72-2332.

†Fannie and John Hertz Foundation Fellow.

[1]R. Z. Sagdeev and A. A. Galeev, *Nonlinear Plasma Theory* (Benjamin, New York, 1969), p. 33.

[2]V. L. Ginzburg, *Propagation of Electromagnetic Waves in Plasma* (Gordon and Breach, New York, 1961), Chap. 4; J. P. Freidberg *et al.*, Phys. Rev. Lett. 28, 795 (1972); M. P. Bachynski *et al.*, Can. J. Phys. 49, 322 (1971); R. L. Stenzel, A. Y. Wong, and H. C. Kim, Phys. Rev. Lett. 32, 654 (1974).

[3]J. D. Lindl and P. K. Kaw, Phys. Fluids 14, 371 (1971). Also observed in recent computer simulations by D. W. Forslund *et al.*, K. G. Estabrook *et al.*, E. J. Valeo *et al.*, and P. Koch *et al.*, presented at Proceedings of the Fourth Annual Symposium on Anomalous Absorption of Intensive High Frequency Waves, Lawrence Livermore Laboratory, April 1974 (to be published).

[4]R. S. Harp, W. B. Cannara, F. W. Crawford, and G. S. Kino, Rev. Sci. Instrum. 36, 960 (1965); P. D. Goldan and W. M. Leavens, Phys. Fluids 13, 433 (1970); P. D. Goldan and E. J. Yadlowsky, Phys. Fluids 14, 1990 (1971).

[5]These features are similar to the results of Valeo *et al.* in Ref. 3, except the amplitudes are larger in their case.

[6]H. C. Kim, A. Y. Wong, and R. L. Stenzel, University of California, Los Angeles, Plasma Physics Group Report No. PPG 177, 1974 (to be published). A similar behavior has been observed by H. Ikezi and K. Nishikawa, Institute of Plasma Physics, Nagoya University, Research Report No. IPPJ-185, 1974 (to be published).

[7]P. Kaw, G. Schmidt, and T. Wilcox, Phys. Fluids 16, 1522 (1973).

[8]A simple physical model of the oscillating two-stream instability based on the ponderomotive force is given by A. Y. Wong and G. Schmidt, Plasma Physics Group, University of California, Los Angeles, Report No. PPG-151, 1973 (unpublished).

[9]K. Nishikawa, J. Phys. Soc. Jpn. 24, 916 (1968); J. R. Sanmartin, Phys. Fluids 13, 1533 (1970).

[10]J. Dawson and T. Lin, private communications.

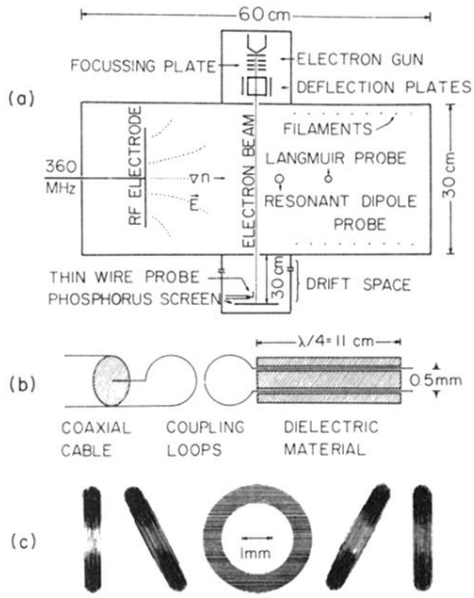


FIG. 1. (a) Schematic diagram of the apparatus, showing plasma device and differentially pumped electron beam device. (b) Resonant-dipole probe consisting of a $\lambda/4$ resonator in a ceramic shield. The potential difference measured between the exposed probe tips is magnetically coupled to a 50-$\Omega$ coaxial cable. (c) Sketches of the observed variation of the Lissajous pattern when the density is increased: (from left to right) $\omega_{pe}^2(z_0)/\omega_0^2 = 0.85$, 0.97, 1.00, 1.03, and 1.10. $P_0 = 10$ W, $\omega_0/2\pi = 360$ MHz, steady state. The horizontal deflection is caused by the plasma field and the vertical deflection by a constant external field.